Response of air stagnation frequency to anthropogenically enhanced radiative forcing

D E Horton *et al*

Supplemental Data

1. SD Methods

We apply the bias correction technique of Ashfaq et al [1,2]. This method adjusts the monthly mean of each climate model parameter to the monthly mean of the observational dataset, while preserving the model-simulated daily variance and time-series autocorrelation of each atmospheric variable, along with the model-simulated change in the monthly-mean and daily distribution between the historic and future periods. Since quantile-based bias correction requires time-series of equal length, we select overlapping periods of late-20th century (1981-2000) from the CMIP3 20C3M simulations, the NCEP/DOE Reanalysis 2 (R2) [3], and the Willmott and Matsuura precipitation dataset [4]. We find that only a small number of CMIP3 models have surface topography that intersects with the 500-mb pressure level, and therefore include 500-mb winds at all grid points. The reanalysis precipitation field is bias corrected (in the same manner as discussed below) using the Matsuura and Willmott [4] precipitation dataset. The NCEP/DOE R2 dataset is a second generation NCEP reanalysis product that incorporates/assimilates observed meteorological variables from the global observational network into a climate model simulation of the recent past, with the purpose of more accurately capturing historic atmospheric conditions [3]. It should be noted that although bias correction of historic model simulations has been shown to substantially improve monthly- and daily-scale model fields [1,2], the correction relies heavily on the veracity of this observational (reanalysis) dataset. Errors in the monthly average observations (reanalysis) will be propagated to both the historic and future bias corrected realizations.

We bias correct each CMIP3 GCM individually. To begin, we interpolate the corresponding reanalysis and late-20th century CMIP3 ensemble member simulation datasets to a common 1.0° × 1.0° latitude-longitude grid, a resolution consistent with the synoptic-scale nature of the ASI and supported by observational analyses of $PM_{2.5}$ concentrations/stagnation correlations in the conterminous U.S. [5]. We then compute the monthly mean value of each variable within each dataset and create ranked quantiles at all grid points (e.g., 20 months of

January ranked from highest to lowest). We adjust the monthly means of the GCM-simulated variables by mapping the reanalysis quantile value to its corresponding GCM quantile. We then distribute this monthly bias correction to the GCM daily time-series; thereby preserving the daily distribution, but ensuring monthly GCM means are equal in magnitude to monthly reanalysis means. For example, to bias correct the daily precipitation fields with monthly mean precipitation:

$$P_c(m,d_m) = [\ P_o(m,d_m) \ / \ P_o(m,\text{ave})\ ] \times P_c(m,\text{ave}) \qquad (1)$$

where $P_c(m,d_m)$ is the bias corrected daily precipitation in month m on day d_m of month m, $P_o(m,d_m)$ is the original model-simulated daily precipitation, $P_o(m,\text{ave})$ is the original model-simulated monthly mean precipitation, and $P_c(m,\text{ave})$ is the bias corrected monthly mean precipitation. To bias correct the 500-mb and 10-m winds, we employ the same procedure.

To apply the historically derived bias correction to the 21st century CMIP3 simulations (SRESA1B), we again begin by interpolating the climate model datasets to the common grid. We then compute the monthly average value of the meteorological variables in both the historic (1981-2000) and future (2081-2100) CMIP3 simulations and create ranked quantiles of each. Using these rankings, we calculate the "quantile shift" from historic-to-future by computing the ratio (future/historic) of the similarly ranked quantile values. The quantile shift represents the model-simulated response to elevated radiative forcing. We multiply the previously calculated bias corrected historic quantiles by their corresponding quantile shift ratios, producing bias corrected future period quantiles for each respective month, i.e.,

$$P_{fc}(m,\text{ave}) = [\ P_f(m,\text{ave}) \ / \ P_h(m,\text{ave})\ ] \times P_{hc}(m,\text{ave}) \qquad (2)$$

where $P_{fc}(m,\text{ave})$ is the future bias corrected monthly mean precipitation in month m, $P_f(m,\text{ave})$ is the model simulated future monthly mean precipitation, $P_h(m,\text{ave})$ is the model simulated historic monthly mean precipitation, and $P_{hc}(m,\text{ave})$ is the historic bias corrected monthly mean precipitation. We distribute these monthly bias corrections to the SRESA1B CMIP3 daily time series, using the same method employed in (1) above, thereby preserving the model-generated daily variance and time-series auto-correlation.

2. SD Figures

Figure S1| Absolute seasonal stagnation changes
(21^{st} - 20^{th} century)

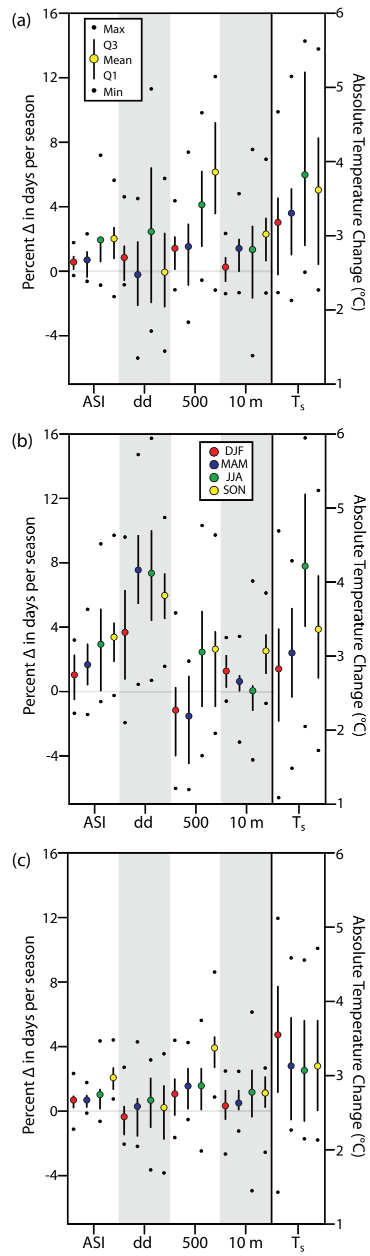

Figure S1. Absolute seasonal stagnation changes of the ensemble members, for (a) the Eastern United States, (b) Mediterranean Europe, and (c) Eastern China and the Korean Peninsula. Y-axis values are the percent change in days per season. Abbreviations: *ASI* – Air Stagnation Index, *dd* – dry days, *500* – 500 mb winds, *10 m* – 10 m winds, and T_S – surface temperature. Statistical abbreviations found in inset (a) are in reference to the CMIP3 ensemble members: *Max* – Maximum simulated value, *Min* – Minimum simulated value, *Q1* – First quartile, *Q3* – Third quartile. Seasons are color-coded and labeled in inset (b). For the corresponding plot in relative change, see Figure 4.

Figure S2| Annual ASI Native 20C3M

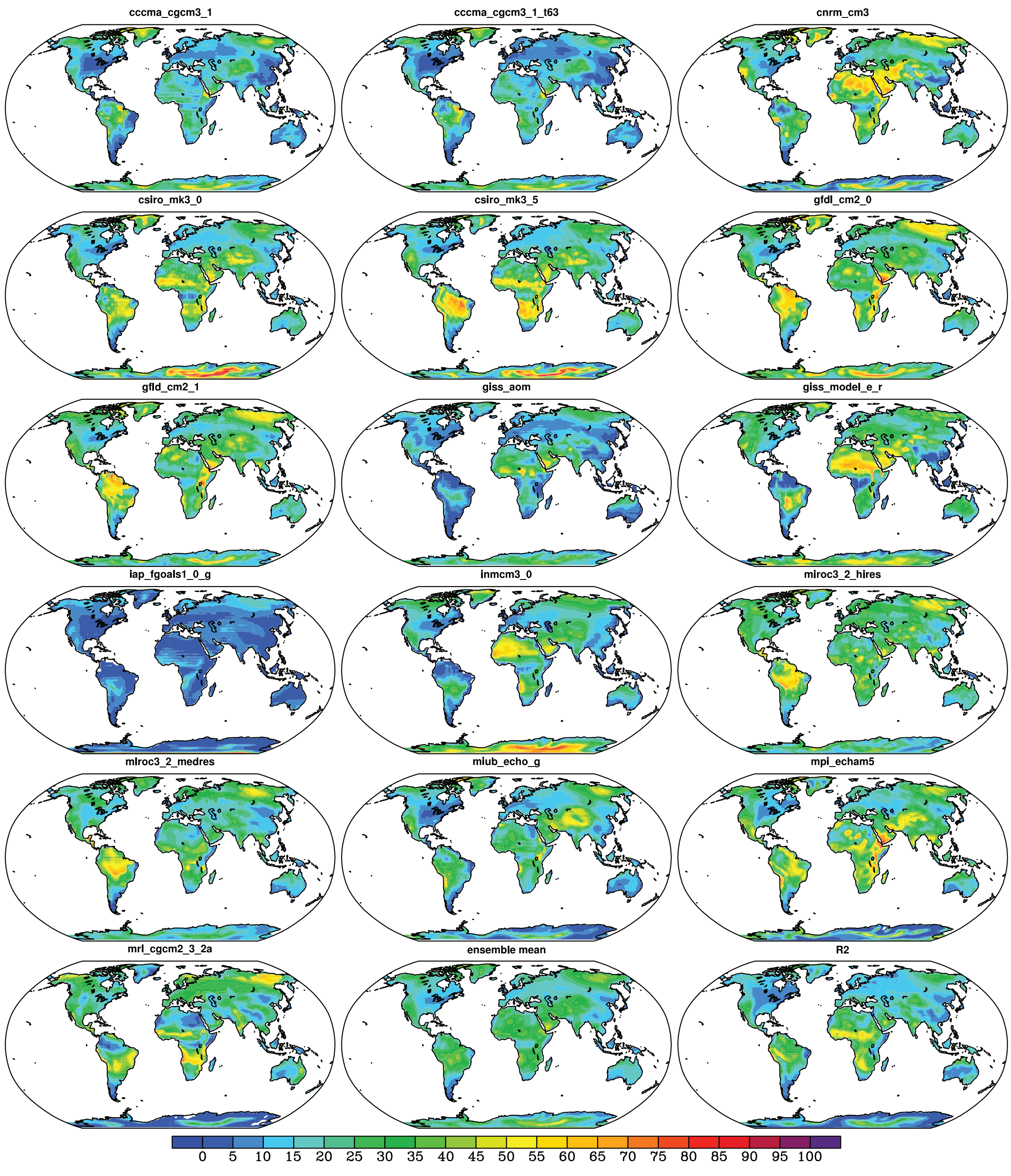

Figure S2. Mean percentage of late-20th century days per year that meet the ASI stagnation thresholds in each native CMIP3 20C3M ensemble member simulation.

Figure S3| Annual ASI Native 20C3M - R2

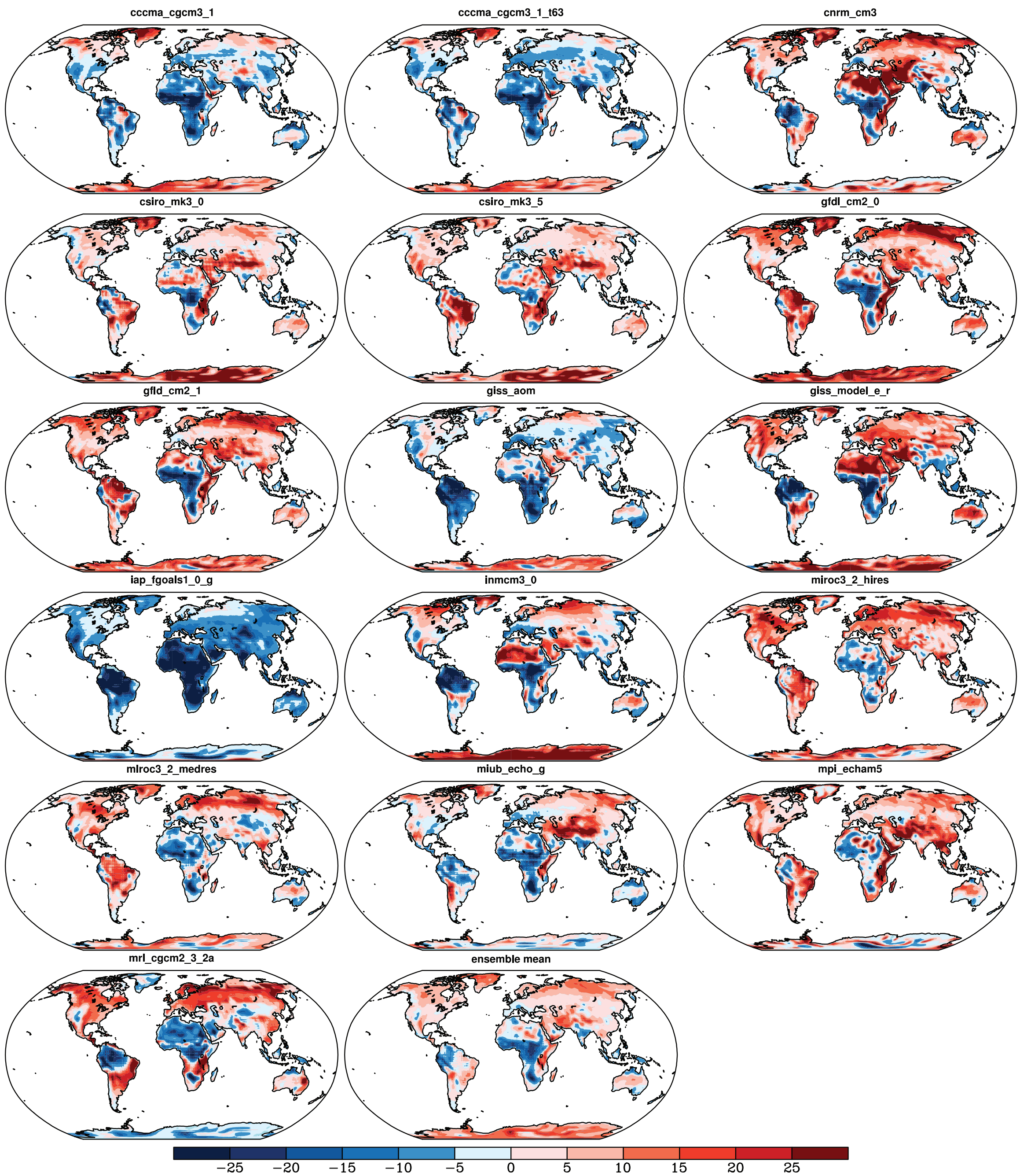

Figure S3. The absolute difference, in percentage of days per year, of late-20[th] century native CMIP3 ensemble member air stagnation occurrence (ASI) and late-20[th] century reanalysis stagnation occurrence (ASI).

Figure S4 Annual ASI Bias Corrected 20C3M

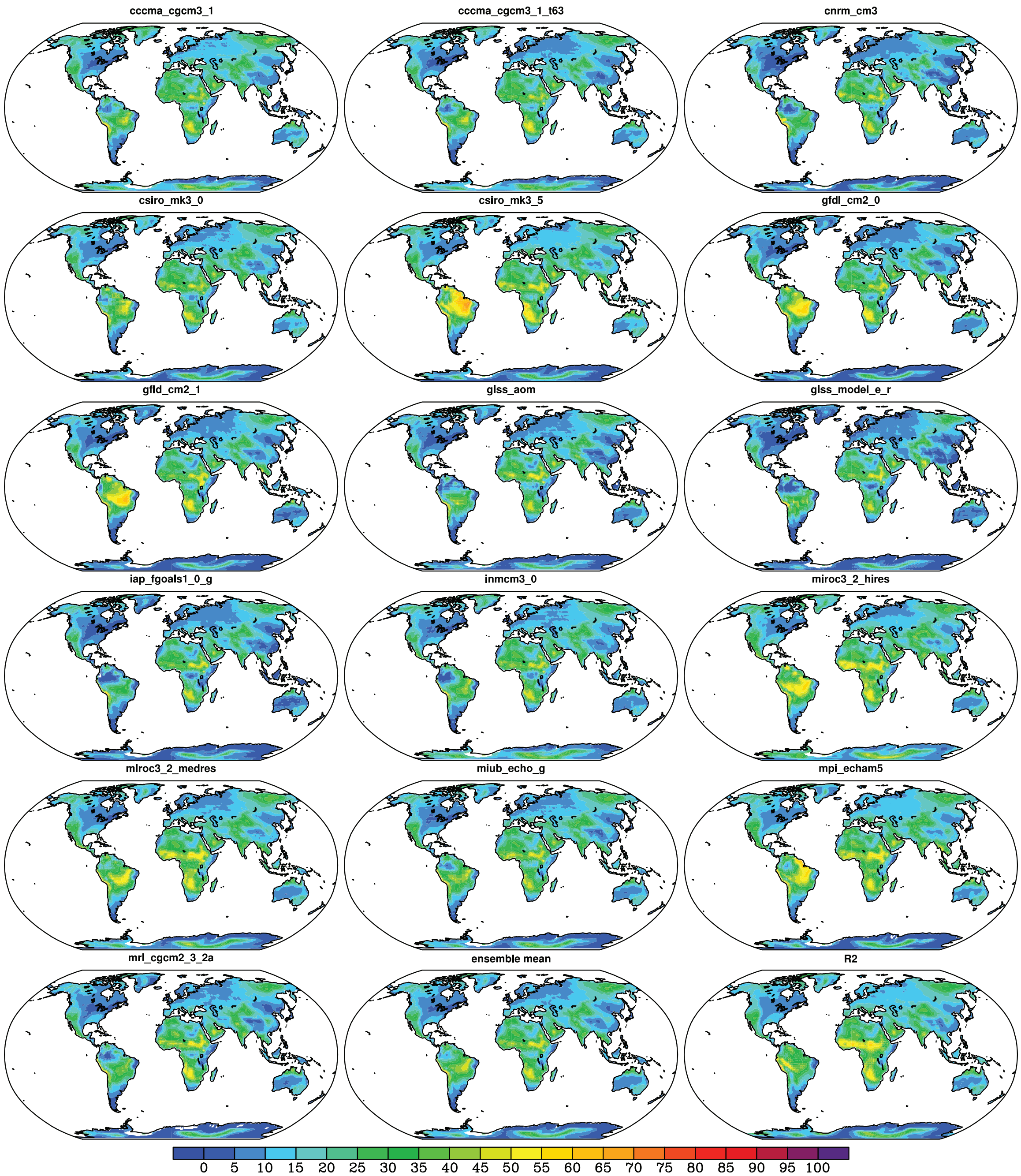

Figure S4. Mean percentage of late-20th century days per year that meet the ASI stagnation thresholds in each bias corrected CMIP3 20C3M ensemble member simulation.

Figure S5| Annual ASI Bias Corrected 20C3M- R2

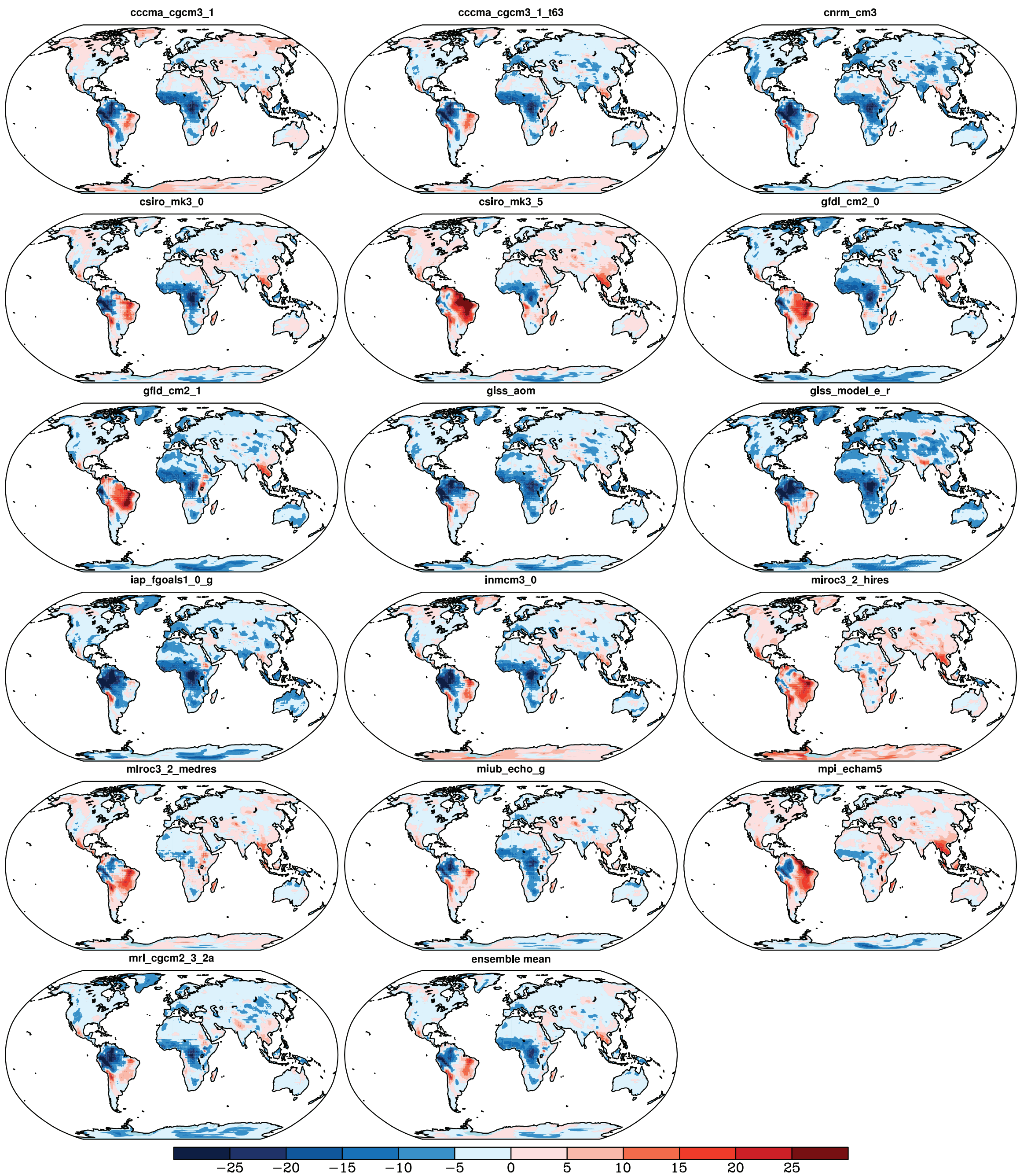

Figure S5. The absolute difference, in percentage of days per year, of late-20th century bias corrected CMIP3 ensemble member annual air stagnation occurrence (ASI) and late-20th century reanalysis annual stagnation occurrence (ASI).

Fig. S6| Annual 500 mb Wind Bias Corrected 20C3M - R2

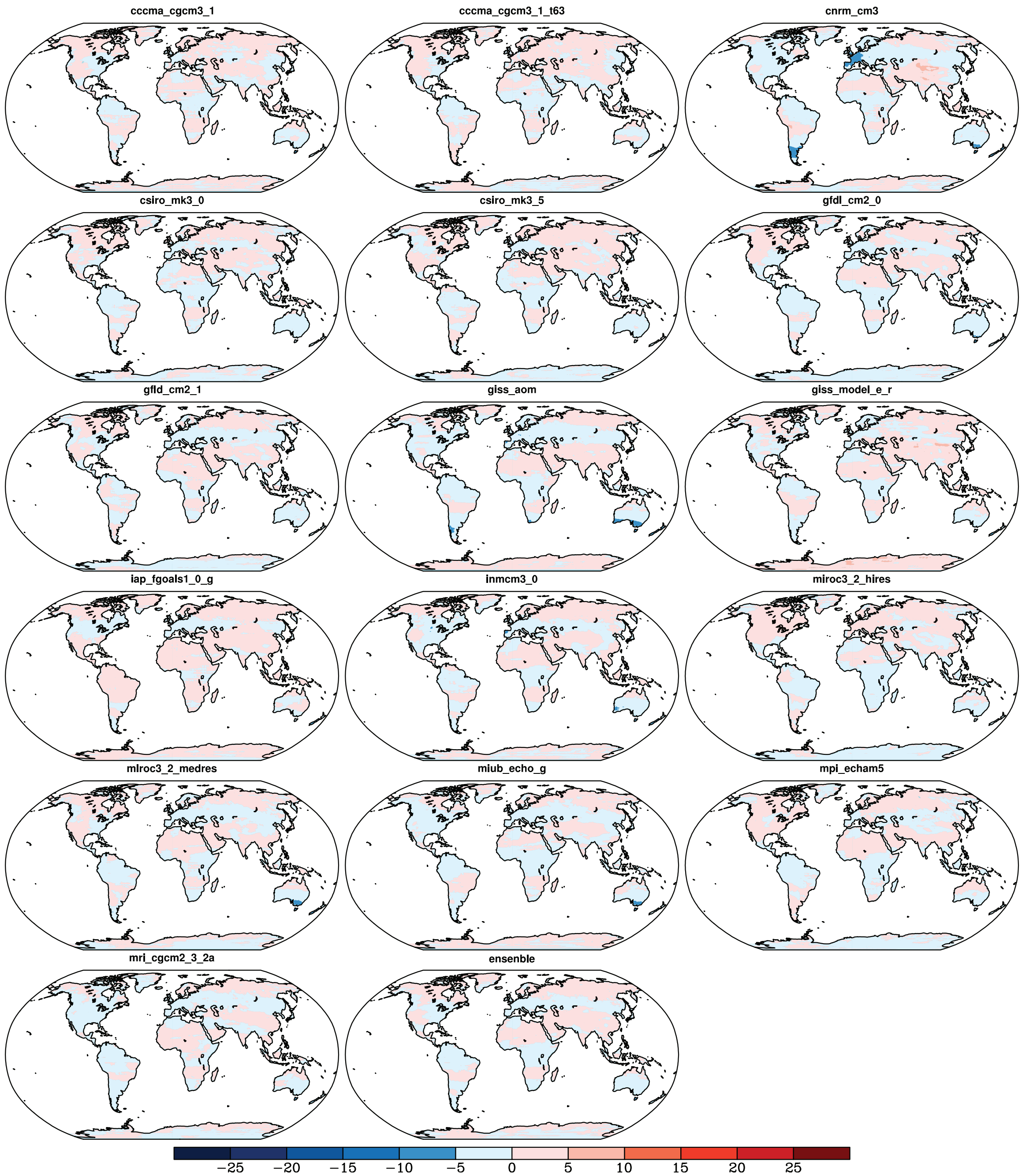

Figure S6. The absolute difference, in percentage of days per year, of late-20th century bias corrected CMIP3 ensemble member annual 500-mb wind stagnation occurrence and late-20th century reanalysis annual 500-mb wind stagnation occurrence.

Fig. S7| Annual 10-m Wind Bias Corrected 20C3M - R2

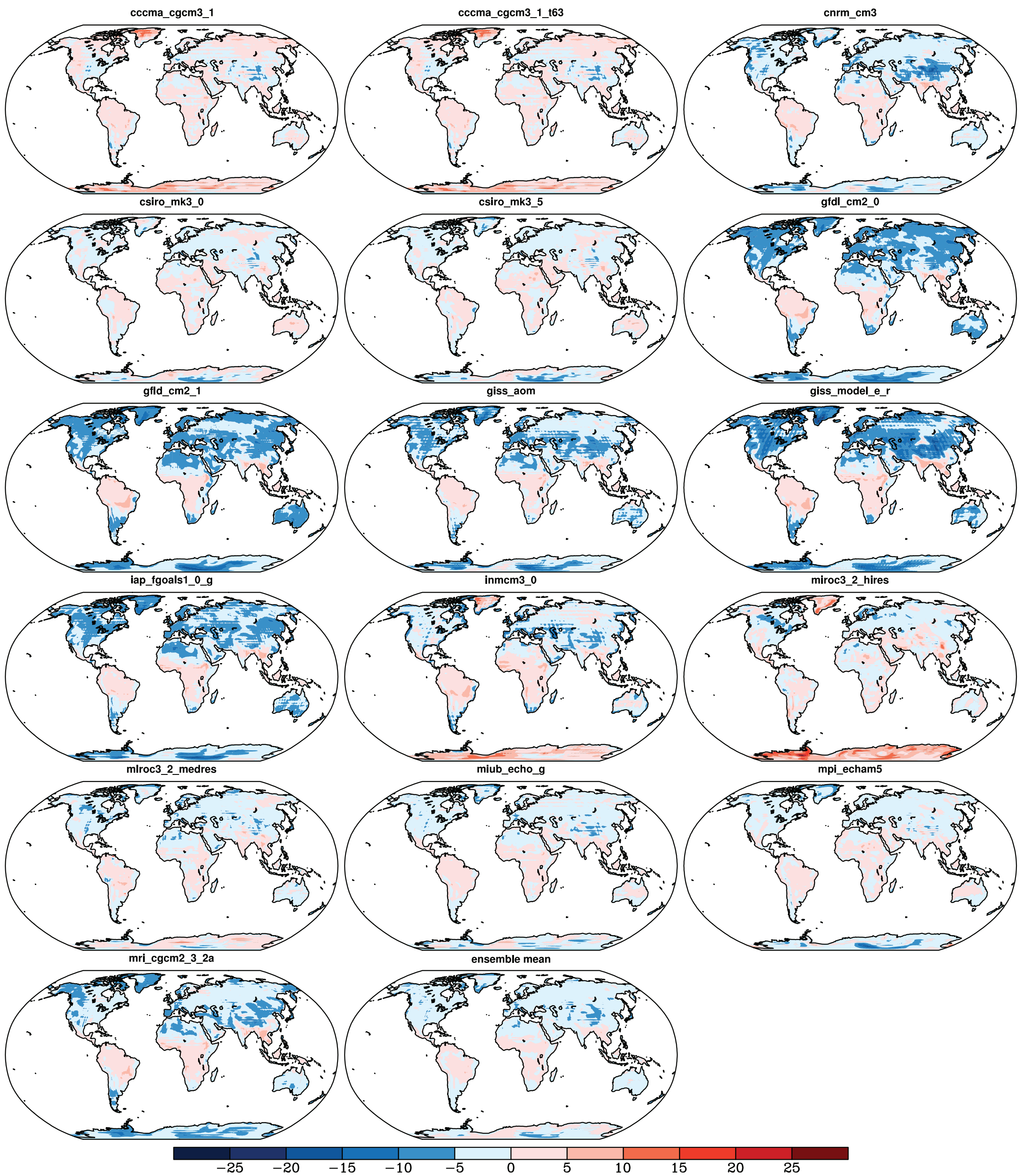

Figure S7. The absolute difference, in percent, of late-20th century bias corrected CMIP3 ensemble member annual 10-m wind stagnation occurrence and late-20th century reanalysis annual 10-m wind stagnation occurrence.

Fig. S8| Annual Dry Days Bias Corrected 20C3M - R2

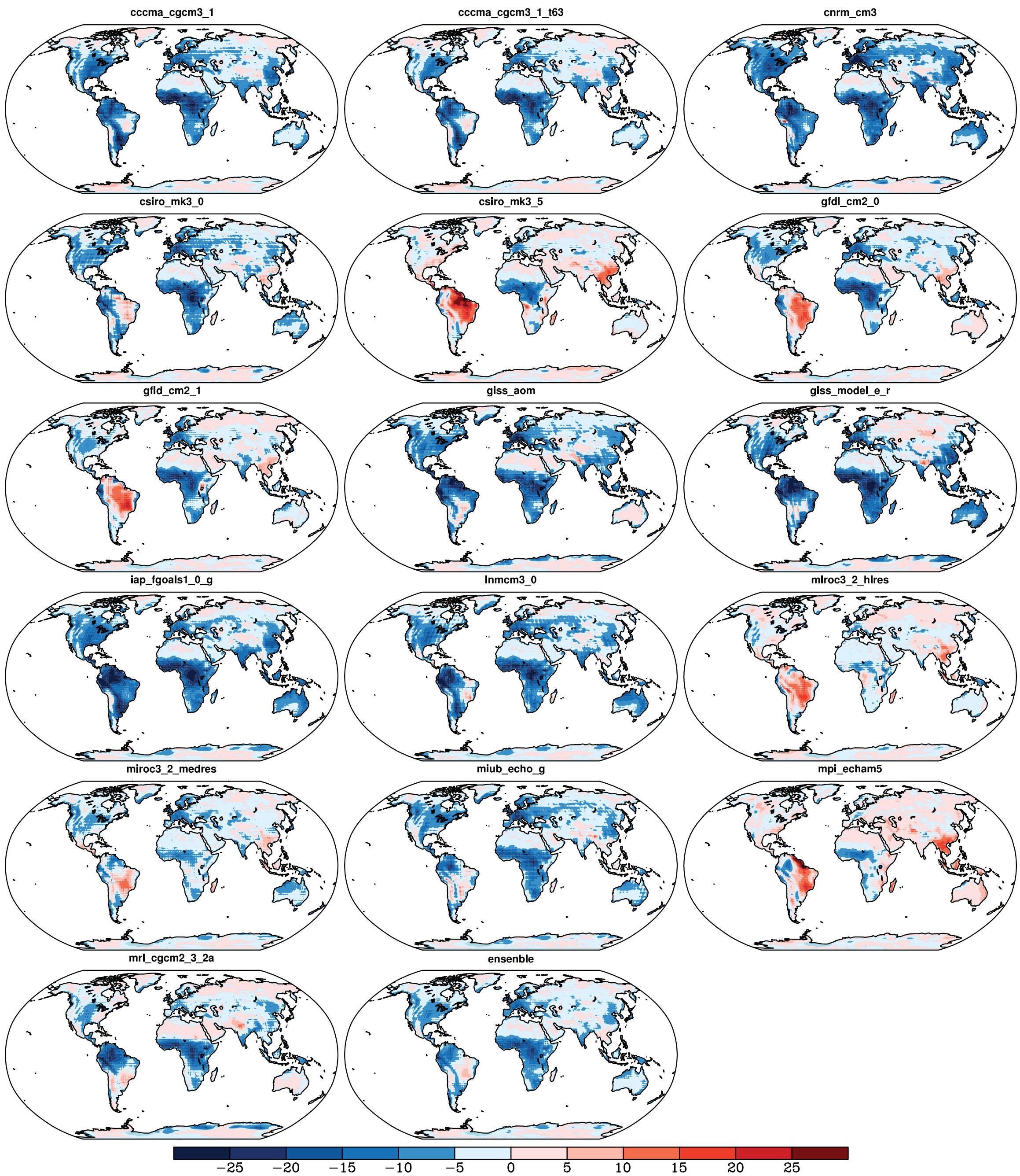

Figure S8. The absolute difference, in percentage of days per year, of late-20th century bias corrected CMIP3 ensemble member annual dry day occurrence and late-20th century reanalysis annual dry day occurrence.

Figure S9| Annual ASI Bias Corrected SRESA1B - Bias Corretced 20C3M

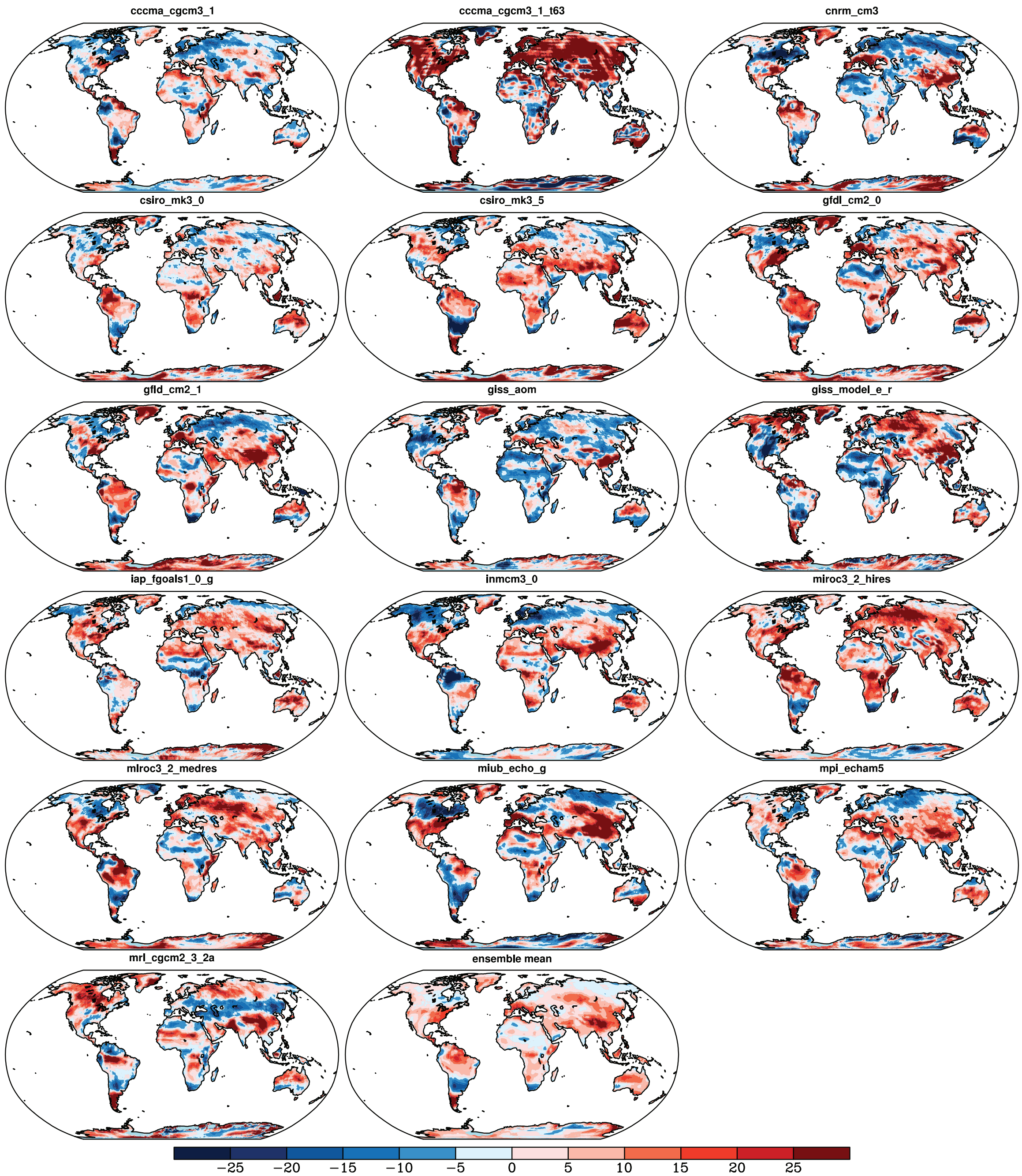

Figure S9. The relative difference, in percentage of days per year, of late-21st century bias corrected CMIP3 ensemble member annual ASI and late-20th century bias corrected CMIP3 ensemble member annual ASI.

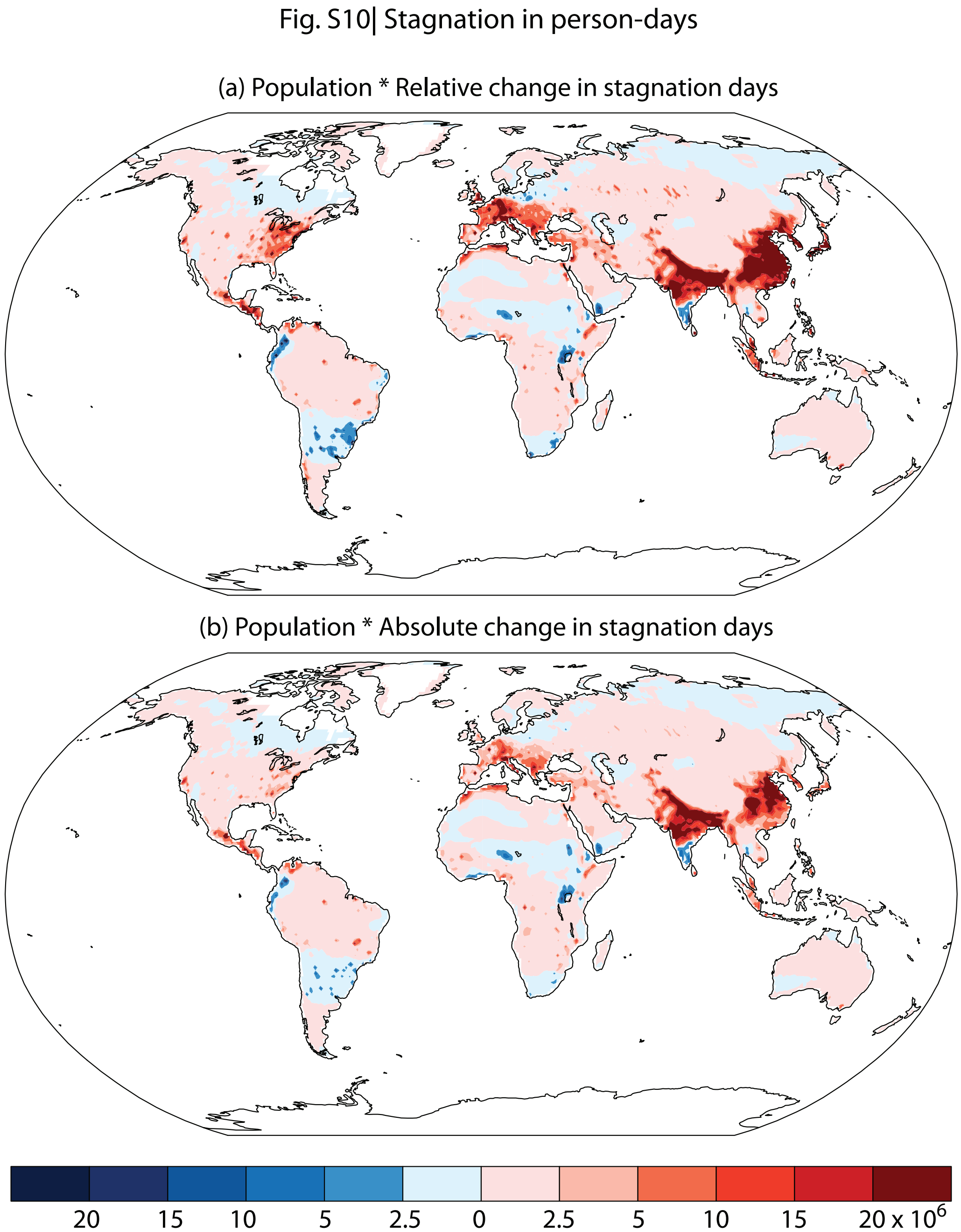

Figure S10. Future changes in simulated ensemble mean annual air stagnation occurrence weighted with year 2000 population counts [6]. (a) Relative change in bias corrected stagnation occurrence from the late-20th to late-21st century (percent change of days/year * population). (b) Absolute change in bias corrected stagnation occurrence from the late-20th to late-21st century (days/year * population). This analysis does not account for population dynamics or changing emissions over the coming century.

CMIP3 Ensemble Members	
IPCC Designation	Resolution
CGCM3.1(T47)	3.8˚x 3.8˚- 9
CGCM3.1(T63)	2.8˚x 2.8˚- 9
CNRM-CM3	2.8˚x 2.8˚- 9
CSIRO-Mk3.0	1.9˚x 1.9˚- 9
CSIRO-Mk3.5	1.9˚x 1.9˚- 9
ECHAM5/MPI-OM	1.9˚x 1.9˚- 9
ECHO-G	3.8˚x 3.8˚- 9
FGOALS-g1.0	3.0˚x 2.8˚- 9
GFDL-CM2.0	2.0˚x 2.5˚-17
GFDL-CM2.1	2.0˚x 2.5˚-17
GISS-AOM	3.0˚x 4.0˚- 9
GISS-ER	4.0˚x 5.0˚- 9
INM-CM3.0	4.0˚x 5.0˚- 9
MIROC3.2(hires)	1.1˚x 1.1˚- 9
MIROC3.2(medres)	2.8˚x 2.8˚- 9
MRI-CGCM2.3.2	2.8˚x 2.8˚- 9

Table S1. CMIP3 ensemble members used in this study, identified via their IPCC designation. Model resolution reported in latitude, longitude, and vertical level. Models were selected based on the availability of daily-scale three-dimensional atmospheric variables from the IPCC 20C3M and SRESA1B simulations found on the U.S. Department of Energy's Program for Climate Model Diagnosis and Intercomparison database.

3. SD References

[1] Ashfaq M, Bowling, Cherkauer K, Pal JS and Diffenbaugh NS 2010a Influence of climate model biases and daily-scale temperature and precipitation events on hydrological impact assessments: A case study of the United States *J. Geophys. Res.* **115** D14116

[2] Ashfaq M, Skinner CB and Diffenbaugh NS 2010b Influence of SST biases on future climate change projections *Clim. Dyn.* doi:10.1007/s00382-010-0875-2

[3] Kanamitsu M, Ebisuzaki W, Woollen J, Yang S-K, Hnilo JJ, Fiorino M and Potter GL 2002 NCEP-DEO AMIP-II Reanalysis (R-2) *Bul. Atmos. Met. Soc.* **83** 1631-43

[4] Tai APK, Mickley LJ and Jacob DJ 2010 Correlations between fine particulate matter ($PM_{2.5}$) and meteorological variables in the United States: Implications for the sensitivity of $PM_{2.5}$ to climate change *Atmos. Envir.* **44** 3976-84

[5] Matsuura K and Willmot CJ 2009 Terrestrial precipitation: 1900-2008 Gridded Monthly Time Series (Version 2.01) [http://climate.geog.udel.edu/~climate/]

[6] Center for International Earth Science Information Network/Colombia University, United Nations Food and Agriculture Programme, and Centro Internacional de Agricultura Tropical 2005 *Gridded Population of the World Version 3: Population Count Grid* (NASA Socioeconomic Data and Applications Center, Palisades, New York).